



ELSEVIER

1 August 2000

Optics Communications 182 (2000) 59–69

OPTICS  
COMMUNICATIONS

www.elsevier.com/locate/optcom

# Aperture apodization using cubic spline interpolation: application in digital holographic microscopy

Etienne Cuche<sup>a,\*</sup>, Pierre Marquet<sup>b</sup>, Christian Depeursinge<sup>a</sup>

<sup>a</sup> *Institute of Applied Optics, Swiss Federal Institute of Technology, CH-1015 Lausanne, Switzerland*

<sup>b</sup> *Institute of Physiology, Laboratory of Neurological Research, Department of Neurology, University of Lausanne, CH-1005 Lausanne, Switzerland*

Received 19 January 2000; received in revised form 15 April 2000; accepted 16 April 2000

## Abstract

A method is proposed for designing apodized apertures with a transmission profile which follows a curve defined using a cubic spline interpolation. The method is applied in digital holographic microscopy to perform digitally the apodization of the aperture of holograms recorded by a CCD camera. The transmission of the apodized aperture is entirely defined by four parameters which are adjusted iteratively to minimize intensity and phase fluctuations appearing in the images obtained by numerical reconstruction of the holograms. The performances of the method have been studied in the absence of experimental sources of noise using a computer generated hologram with which we demonstrate that the aperture apodization reduces the standard deviation of the reconstructed phase distribution from 1.6 nm to 0.15 nm. © 2000 Elsevier Science B.V. All rights reserved.

PACS: 42.15; 42.40; 42.25.F; 42.50.D

Keywords: Apodization; Cubic spline interpolation; Digital holography

## 1. Introduction

In coherent optics, when an aperture truncates a light beam in an imaging system, diffraction by the edge of the aperture induces spatial fluctuations of the transmitted optical field. In laser amplification for example such fluctuations of the intensity must be avoided because they may cause bulk damages to the amplifying media. A solution to this problem

consists in using so-called apodized apertures which are characterized by a transmission which does not change abruptly from zero to unity at the edge of the aperture, but in a smooth and continuous manner. The question of aperture apodization has been studied in details in the past years [1–5] and several kinds of functions, such as Gaussian, super-Gaussian or trigonometric functions have been proposed to define the transmission of an apodized aperture. However, finding the optimal shape for the curve describing the transition of the transmission at the edge of the aperture is a complicated task which is

\* Corresponding author. Fax: +41-21-693-3730; e-mail: etienne.cuche@epfl.ch

difficult to achieve using analytical functions. As shown by Tommasini et al. [6], the definition of transmission profiles using numerical iterative methods offers an interesting solution to this problem.

In this paper we propose a new, to our knowledge, method in which the transmission profile of the aperture follows a curve defined by a cubic spline interpolation. The advantage of this approach is that a broad variety of continuous curves can be defined with only few parameters. In the case presented here, the two-dimensional (2D) transmission of the apodized aperture is entirely defined by four parameters and the shape of the apodization is optimized by adjusting iteratively the values of these parameters.

Although the method presented here can be applied generally for designing apodized apertures, the present paper discusses only a particular application within the framework of digital holographic microscopy (DHM) [7,8]. The designation DHM applies here to an emerging family of imaging techniques involving a Charged Coupled Device (CCD) for recording of a digital hologram of the specimen and a numerical method for the hologram reconstruction. Up to now, the terms digital holography or numerical holography have been used in the literature to designate this type of imaging procedures. But in this case, a confusion may arise with other techniques in which numerical means are used to create a so-called computer generated hologram (CGH). An attractive feature of DHM is that an amplitude-contrast image and a phase-contrast image of the specimen can be obtained simultaneously with only one hologram acquisition. As shown in Ref. [7] where an application to surface profilometry is presented, the reconstructed phase distribution provides a quantitative and precise information about the three-dimensional structure of the specimen surface.

The link between the problem of aperture apodization and the DHM method is that diffraction effects play an important role in the numerical reconstruction process of the DHM method. As shown here, due to the finite size of the hologram aperture, high frequency intensity and phase fluctuations appear in the form of fringes along the edges of the images. These fluctuations introduce artifacts in the reconstructed images and reduce their quality. Phase fluctuations in particular are disturbing for the potential applications of the method in optical metrology.

We show here that these diffraction effects can be reduced by digital apodization of the hologram aperture.

Another objective is to address the question of phase measurements with the DHM method. We show that, after apodization of the hologram aperture, the reconstructed images contain a central region in which fluctuations produced by diffraction effects becomes negligible. A quantitative evaluation of the resolution limit of the DHM method for phase measurements can be obtained by measuring the standard deviation of the reconstructed phase distribution in this central region. A first estimation of the resolution limit has been performed in the absence of experimental noise using a computer generated hologram. In this case, the standard deviation gives an estimation of the noise associated to the numerical reconstruction method. A preliminary experimental study shows that this reconstruction noise is much smaller than the experimental noise.

The paper is organized as follows. In Section 2 we present a short description of the DHM method. Section 3 illustrates the consequences of diffraction effects in the numerical reconstruction process and Section 4 describes the method used to define the transmission of the apodized aperture. Section 5 presents the results and gives an estimation of the resolution limit of the DHM method for phase measurements. Concluding remarks can be found in Section 6.

## 2. Digital holographic microscopy (DHM)

Refs. [7,8] give a detailed description of the numerical reconstruction method and describe three different experimental arrangements which can be used to record off-axis holograms using a CCD camera. Applications of similar techniques can be found in Refs. [9–15]. A short description is given here as a reminder. It corresponds to the configuration presented in Ref. [7]. It is however clear that the method of aperture apodization which is presented in this paper can also be applied to holograms recorded using other configurations, and in particular those for holographic microscopy that are presented in Ref. [8].

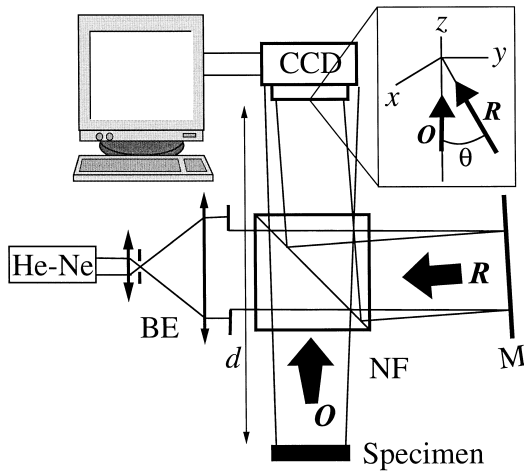


Fig. 1. Experimental setup: BE beam expander, M mirror,  $O$  object wave,  $R$  reference wave. Inset: a detail showing the off-axis geometry.

A diagram of the experimental setup is illustrated in Fig. 1. Linearly polarized plane wave fronts are produced by a beam expander BE including a pinhole for spatial filtering. A 15 mW He–Ne laser is used as light source. At the exit of the interferometer a CCD camera records the hologram which results from the interference between the object wave  $O$  and the reference wave  $R$ . As shown inset in Fig. 1, the reference wave reaches the CCD with an incidence angle  $\theta$  in order to obtain off-axis holograms. As explained for example in Ref. [10], the  $\theta$  value must be small enough to avoid that the carrier frequency of the interferogram exceeds the resolving power of the CCD camera. Digital holograms containing  $N \times N = 512 \times 512$  pixels encoded with 256 gray levels are transmitted to a computer. The area of the CCD chip is  $L \times L = 4.85 \times 4.85 \text{ mm}^2$ .

The numerical method for hologram reconstruction consists basically in computing the Fresnel diffraction pattern of the hologram. The reconstructed wave front  $\Psi(m,n)$  is obtained using the following algorithm [7,8]:

$$\Psi(m,n) = A \exp\left(\frac{i\pi}{\lambda d}(m^2 \Delta \xi^2 + n^2 \Delta \eta^2)\right),$$

$$FFT\left[\mathbf{R}_D(k,l) I_H(k,l) \exp\left(\frac{i\pi}{\lambda d}(k^2 \Delta x^2 + l^2 \Delta y^2)\right)\right]_{m,n}, \quad (1)$$

where  $k,l,m,n$  are integers ( $-N/2 \leq k,l,m,n < N/2$ ),  $I_H(k,l)$  is the digital hologram which results from the 2D spatial sampling and from the digitizing of the hologram intensity by the CCD camera,  $FFT$  is the fast Fourier transform operator,  $\lambda$  is the wavelength (632.8 nm), and  $A = \exp(i2\pi d/\lambda)/(i\lambda d)$  is a constant. The parameter  $d$  represents the distance between the hologram plane  $0xy$  and the observation plane  $0\xi\eta$ . To obtain in-focus reconstructed images, the  $d$  value must be equal to the object–CCD distance (see Fig. 1).  $\Delta x$  and  $\Delta y$  defines the sampling intervals in the hologram plane ( $L/N$ ). The sampling intervals in the observation plane ( $\Delta \xi$  and  $\Delta \eta$ ) are defined by the size of the CCD ( $L$ ) and by the distance  $d$  [8]:

$$\Delta \xi = \Delta \eta = \frac{\lambda d}{L}. \quad (2)$$

Relation (2) defines the transverse (or lateral) resolution of the DHM method when experimentally implemented with configuration presented in Fig. 1. One can see that this transverse resolution increases with the specimen–CCD distance ( $d$ ) and decreases with the aperture size of the detector ( $L$ ).

The reconstructed wave front  $\Psi(m,n)$  is an array of complex numbers which represents a digital replica of the complex amplitude of the wave front that would have been diffracted by the hologram during a standard optical reconstruction. Two images of the specimen can be obtained from this numerically reconstructed wave front. A first image, called amplitude-contrast image  $I(m,n)$ , can be obtained by calculating the distribution of intensity in the observation plane:

$$I(m,n) = |\Psi(m,n)|^2 = \text{Re}(\Psi(m,n))^2 + \text{Im}(\Psi(m,n))^2, \quad (3)$$

where  $\text{Re}(\Psi(m,n))$  is the real part of the reconstructed wave front and  $\text{Im}(\Psi(m,n))$  its imaginary part. A second image, called phase-contrast image  $\phi(m,n)$ , which represents the phase distribution at the surface of the specimen, can be obtained by calculating the argument of  $\Psi(m,n)$ :

$$\phi(m,n) = \arctan\left(\frac{\text{Im}(\Psi(m,n))}{\text{Re}(\Psi(m,n))}\right). \quad (4)$$

It is an interesting feature of the DHM method that these two images of the specimen can be obtained simultaneously, on the basis of a single hologram acquisition.

In Eq. (1),  $R_D(k,l)$  is a computed array of complex numbers called digital reference wave. For phase-contrast imaging [7,8], this digital reference wave must be a precise replica of the experimental reference wave  $R$ . When  $R$  is a plane wave,  $R_D(k,l)$  is calculated as follows:

$$R_D(k,l) = \exp\left(i \frac{2\pi}{\lambda} (k_x k \Delta x + k_y l \Delta y)\right), \quad (5)$$

where  $k_x$  and  $k_y$  are two parameters which must be precisely adjusted to obtain a phase-contrast image of the specimen. A description of the procedure used for the adjustment these two parameters can be found in Ref. [8].

As with classical holography, the reconstructed wave front contains three different terms: a real image, a virtual image and a zero order of diffraction. These terms can be observed separately as a consequence of the off-axis geometry. Reconstructed images presented in this paper do not show the entire area of the observation plane, but only a region of interest which contains the real image.

### 3. Diffraction effects in DHM

The numerical reconstruction method used in DHM (Eq. (1)) computes the Fresnel diffraction of a hologram defined in an finite size aperture. As generally in coherent optics, diffraction occurring at the edges of the aperture induces fluctuations of the reconstructed wave front. A typical illustration of this phenomenon can be found in Fig. 2(b) and 2(c). We demonstrate here that these diffraction effects can be reduced by apodization of the hologram aperture.

It is important to realized that fluctuations of the reconstructed wave front may have many other origins than diffraction effects. In practice, vibrations, turbulences, dust, flatness defects and optical aberrations introduce noise and artifacts in the reconstructed images. As the diffraction effects that we want to consider here arise during the numerical reconstruction process, these contributions must be

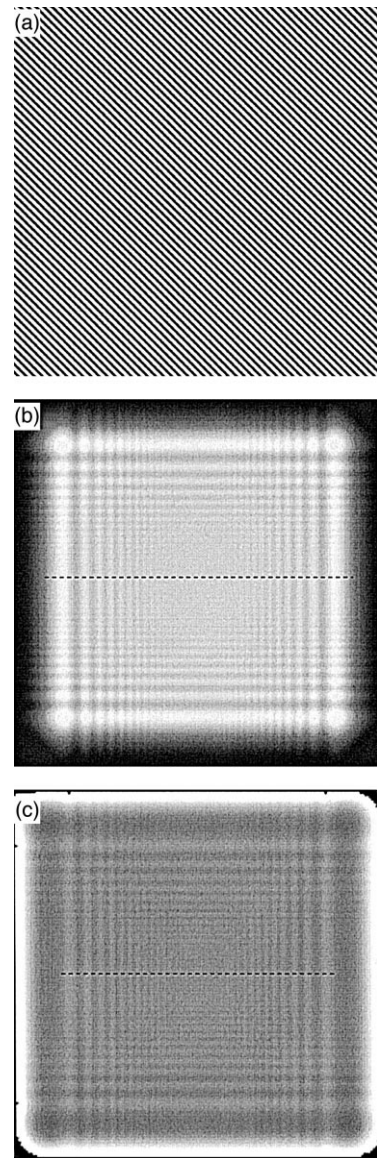


Fig. 2. Diffraction effects in digital holographic microscopy: (a) computed hologram resulting from the interference of two plane waves; (b) numerically reconstructed amplitude-contrast image; and (c) phase-contrast image. The dashed lines indicates the position of the profiles presented in Figs. 5 and 6.

eliminated for designing the apodized aperture in the absence of experimental sources of noise. For this reason, the application of our apodization method in DHM has been tested using a computer generated hologram which is presented in Fig. 2(a). This com-

puted off-axis hologram is a 2D sinusoidal intensity pattern resulting from the interference between two plane waves having different propagation directions. The reconstruction of such an ideal hologram should produce a plane wave as reconstructed wave front, and as consequence, a real image with constant and uniform distributions of intensity and phase. However, as shown in Fig. 2(b) and 2(c), high frequency fluctuations in the form of fringes appearing along the edges of the reconstructed images, can be observed in both intensity and phase. The reconstructed images have been obtained for a reconstruction distance  $d = 30$  cm. As already mentioned Fig. 2(b) and 2(c) do not present the entire area of the observation plane but only a region of interest (in this case  $170 \times 170$  pixels) which contains the real image. The area of the presented images ( $5.0 \times 5.0$  mm<sup>2</sup>) can be calculated using Eq. (2) which gives the pixel size in the observation plane.

These two images simply reveal the Fresnel diffraction pattern of the hologram aperture. These diffraction effects damage image quality and decrease the resolution of the method for phase measurements which are of particular interest for metrological applications of the DHM method.

#### 4. Apodization with cubic spline interpolation

Apodization of the hologram aperture could be achieved experimentally by inserting an apodized aperture in front of the CCD. However, as a digital image of the hologram is acquired, it is more practical to perform this operation digitally by multiplying the digitized hologram intensity with a 2D function representing the transmission of the apodized aperture. A profile of this function is presented in Fig. 3. The aperture is completely transparent (transmission equal to unity) in a large central part ( $\sim 60\%$ ) of the profile. At the edges, the transmission vary from zero to unity following a curve defined by a cubic spline interpolation.

The transmission profile presented in Fig. 3 is similar to the so-called Tukey window which is sometimes used for band-pass filtering in signal processing. The difference is that with the Tukey window, the cubic spline interpolation is replaced by the half period of a sine function. In comparison with

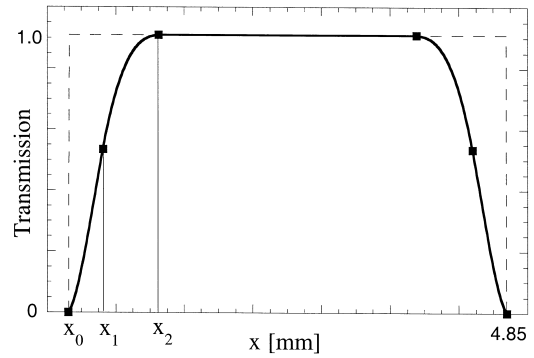


Fig. 3. Transmission profile of the apodized aperture. The transition from 0 to 1 at the edge of the aperture follows a cubic spline interpolation defined by three points (square dots). The dashed line indicates the transmission of the unapodized aperture.

Gaussian apodization, this kind of apertures presenting a large transparent area are interesting from the point of view of energy transfer. In our case, and in particular for amplitude-contrast imaging, apodization using functions with a narrow transparent area must be avoided because the reconstructed intensity distribution is also apodized with a similar transmission profile.

Three points, indicated by square dots in Fig. 3, define the interpolated curve. The values of the first derivative at the extremities of the curve are also required to calculate the cubic spline interpolation. Let's define  $T(x)$  the interpolated function which defines the transition of the transmission,  $T'(x)$  its first derivative and  $\{x_0, x_1, x_2\}$  a set of three points (see Fig. 3), where the values of the function  $\{T(x_0), T(x_1), T(x_2)\}$  are defined. The coordinate of the first point and the value of the function in this point are both fixed to zero ( $x_0 = 0.0$  and  $T(x_0) = 0.0$ ). At the end of the transition curve ( $x = x_2$ ), the value of the function is set to unity ( $T(x_2) = 1.0$ ) and its first derivative is set to zero ( $T'(x_2) = 0.0$ ). The first derivative at the origin of the curve ( $T'(x_0)$ ), the coordinates  $x_1$  and  $x_2$  and the value of the function in the second point  $T(x_1)$  form a set of four parameters which define the shape of the curve. The transmission profile is symmetric with respect to the center of the aperture and the transition at the other side of the aperture (on the right in Fig. 3) is defined by transposing the array containing the interpolated

values of  $T(x)$ . Finally, the same transmission profile is applied along the  $0y$  direction to obtain a 2D function:  $T(x, y) = T(x)T(y)$ . In summary, the aperture is entirely defined by four constrains:  $x_0 = 0$ ,  $T(x_0) = 0$ ,  $T(x_2) = 1.0$ ,  $T'(x_2) = 0.0$  and by four adjustable parameters:  $T'(x_0)$ ,  $x_1$ ,  $x_2$ ,  $T(x_1)$ .

An iterative process has been applied to define the transmission profile presented in Fig. 3. A loop comprising the apodization of the hologram presented in Fig. 2(a) and its numerical reconstruction using Eq. (1) has been implemented. At the beginning of each iteration, the shape of the apodization can be modified by changing the values of  $T'(x_0)$ ,  $x_1$ ,  $x_2$  and  $T(x_1)$ . The goal is of course to adjust these parameters in order to minimize the fluctuations of the reconstructed wave front. In a first approach, these parameters have been adjusted empirically and the fluctuations were simply evaluated by visual inspection of the reconstructed images. A more accurate evaluation can be achieved on the basis of intensity and phase profiles such as those presented in Figs. 5 and 6. It is also possible to obtain a quantitative evaluation of the fluctuations by calculating the standard deviation of the reconstructed intensity or phase distributions. As explained in the next section, the standard deviation is not calculated for the entire area of the reconstructed images but only in a central region where diffraction effects becomes negligible as a result of the hologram apodization. Excellent results, with standard deviations smaller than  $0.2^\circ$  for the phase distribution, have been obtained rapidly using this empirical method of adjustment.

In a second step, an optimization process has been applied in order to minimize the phase fluctuations. Small intervals have been defined around the values previously obtained for  $T'(x_0)$ ,  $x_1$ ,  $x_2$  and  $T(x_1)$  and a standard numerical iterative method (golden section search, see e.g. Ref. [16]) has been used for automatic adjustment. The search of the optimal value, i.e. the value which minimize the standard deviation of the reconstructed phase distribution, has been performed several time for each parameter up to the measured standard deviation remains constant. The values obtained at the end of this procedure are the following:  $T'(x_0) = 0.51$ ,  $x_1 = 0.677$  mm,  $x_2 = 1.042$  mm and  $T(x_1) = 0.65$ . Of course, these values depends on the aperture size ( $L = 4.85$  mm).

The application of an empirical method of adjustment prior to the application of the automatic one permits to restrict the intervals for the search of the optimal values. This point is important because the dependence between the field fluctuations and the

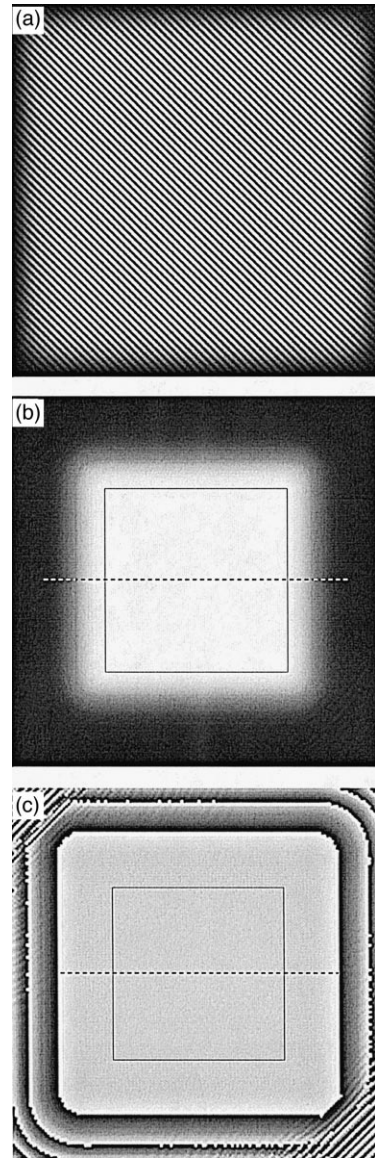


Fig. 4. (a) Apodized hologram; (b) numerically reconstructed amplitude-contrast image; and (c) phase-contrast image. The dashed lines indicate the position of the profiles presented in Figs. 5 and 6. Square area defined with solid lines delimitate regions where diffraction effects are negligible.

shape of the apodization is a complicated function which presents several local minima. Another advantage is that it reduces the number of iterations required to reach the convergence.

The transmission profile presented in Fig. 3 minimize the phase fluctuations but the optimization process can also be performed for others criteria. For example in order to maximize the energy transfer with a fixed amount of intensity fluctuations. It is also important to point out that the transmission profile obtained here is optimized for a plane wave illumination. For another kind of wave front, e.g. a Gaussian beam, the aperture design has to be adapted. Another point is that in most cases, apodized apertures are circular because they are inserted in imaging systems with a cylindrical symmetry. In this case, the method presented here can also be applied by defining a 2D transmission of the form  $T(r)$  with  $r = \sqrt{x^2 + y^2}$ . The use of circular apertures has been tested in the context of the DHM method in order to study the influence of the aperture shape, and in particular to study if the corners of a square aperture introduce diffraction effects. No significant changes have been observed, probably because the corners of the aperture are smoothed by apodization (see Fig. 4(a)).

## 5. Results and discussion

Fig. 4(a) shows the result obtained by application of the apodization procedure, described in Section 4,

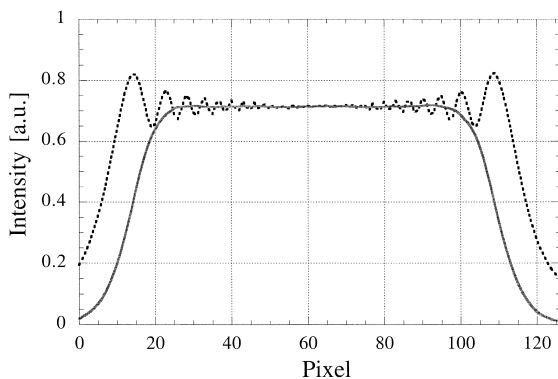


Fig. 5. Normalized intensity profiles (in arbitrary units [a.u.]) extracted from the amplitude-contrast images reconstructed from the unapodized hologram (dotted) and from the apodized hologram (solid).

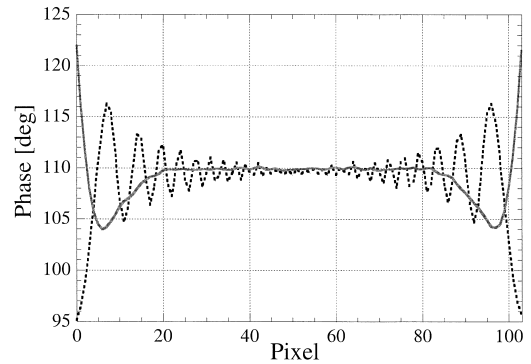


Fig. 6. Phase profiles extracted from the phase-contrast images reconstructed from the unapodized hologram (dotted) and from the apodized hologram (solid).

to the hologram presented in Fig. 2(a). A progressive decrease of intensity can be observed at the edges of the image. The amplitude-contrast and phase-contrast images obtained by numerical reconstruction of the apodized hologram are presented in Fig. 4(b) and 4(c) respectively. The comparison with Fig. 2(b) and 2(c) shows that the high frequency Fresnel modulations of the reconstructed wave front are strongly reduced by apodization.

The effects of apodization can be analyzed more precisely in Figs. 5 and 6 where profiles extracted from the reconstructed distributions of intensity and phase are presented. The dotted plots correspond to the results obtained without apodization and the solid plots to the results obtained with apodization. In the amplitude-contrast images of Fig. 2(b) and 4(b), dashed lines indicate the position of the extracted intensity profiles. In the phase-contrast images of Fig. 2(c) and 4(c), dashed lines indicate the position of the extracted phase profiles.

One can see that the wave front reconstructed from the apodized hologram is not a perfect plane wave over the entire area of the obtained images. However, regions with approximately constant distributions of intensity and phase can be defined in the center of the images. From Fig. 5, we can see that this region extends between the 25th and the 95th pixels in the intensity profile. In Fig. 6, we can see that the region with a constant phase distribution extends between the 20th and the 80th pixels. The

corresponding areas in the reconstructed images are indicated by squares delimited with a thin solid lines in Fig. 4(b) and 4(c).

The area of these central regions with constant distributions is proportional to the area of the apodized window which is completely transparent. For this reason, attention has been paid to keep the  $x_2$  value (see Fig. 3) small with respect to the aperture size ( $L$ ) in order to minimize the width of the segment where the transmission vary from zero to unity.

As can be seen in Fig. 5, apodization leads to a shrinking of the amplitude-contrast image. In Fig. 6, we can see that large oscillations remain outside the central region, but with a reduced frequency which is less disturbing for imaging purposes. In Fig. 4(c), phase jumps (from  $-\pi$  to  $\pi$ ) can be observed at the edges of the image.

From the point of view of the DHM method, the regions defined above in the center of the reconstructed images can be considered as areas where diffractions effects becomes negligible as a result of the hologram apodization. The measurement of the standard deviation in these area has been used to evaluated quantitatively the fluctuations of the reconstructed distributions during the optimization process (see Section 4).

Since Fig. 4(b) and 4(c) have been obtained in the absence of experimental sources of noise, from a computed generated hologram, fluctuations remaining in the central regions defined above can be considered as representing the contribution of the numerical reconstruction procedure to the noise of the entire imaging method. In the central region delimited by a solid line in Fig. 4(c), the standard deviation of the phase distribution is 0.089 degree. This reconstruction noise defines the resolution limit of the method for phase measurements in the absence of experimental sources of noise and corresponds to an optical path length (OPL) of about 0.15 nm at a wavelength of 633.8 nm. For comparison, without apodization, the standard deviation measured in the same region in Fig. 2(c) is approximately one order of magnitude higher (0.904 degree corresponding to an OPL of 1.6 nm).

The resolution limit of 0.15 nm for phase measurements has been verified numerically by shifting the phase of the object wave used to calculate the

computer generated hologram. It has been verified that if the introduced phase shift is equal to the expected resolution limit, the mean value of the reconstructed phase distribution is also shifted with the same amount which can be distinguished from the reconstruction noise.

At the detection level, a phase shift of the object wave results in a translation of the interference fringes. Therefore, the resolution of the method for phase measurements depends essentially on the ability of the CCD camera to detect fringes translations. Several parameters such as the contrast and the carrier frequency of the fringes, as well as the pixel size and the dynamic range of the CCD influence the resolution limit. The exact impact of these parameters has not been exactly established for the moment.

Fig. 7 is presented here to illustrate the effects of apodization in an experimental case. A hologram has been recorded using the setup presented in Fig. 1 with a mirror as specimen. In Fig. 7(a) which presents the phase-contrast image reconstructed without apodization, diffractions effects are clearly observable and we can see in Fig. 7(b) that they are significantly reduced by apodization. Although the effects of apodization are clear on the visual appearance of the reconstructed images, they are less marked in a quantitative point of view because the standard deviation of the phase distribution is reduced from  $4.47^\circ$  ( $\sim 7.8$  nm) in the unapodized case to  $2.87^\circ$  ( $\sim 5.0$  nm) in the apodized case. This large difference in comparison with the results obtained with the computer generated hologram are of course due to phase fluctuations introduced by experimental sources of noise.

As with all interferometric techniques, mechanical vibrations and air turbulences are two important sources of noise the effects of which can be reduced by an appropriate mechanical design and by decreasing the duration of the interferogram acquisition. Another important source of noise comes from fluctuations that are produced by optical errors resulting from design, fabrication or alignment imperfections. In this case, the produced fluctuations are fixed in time and can be reduced by optimizing the optical design and by the use of high-quality optics components. Edge diffraction produced by apertures in the experimental setup and parasitic reflections also contribute to the experimental noise. It is also important

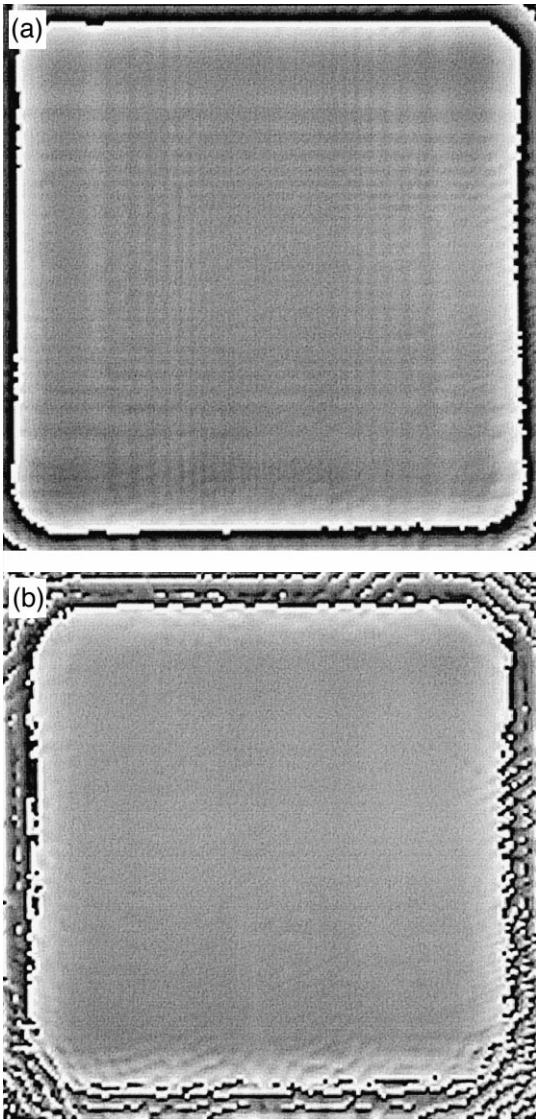


Fig. 7. Phase-contrast images obtained by numerical reconstruction of a hologram recorded experimentally using a mirror as specimen: (a) Without apodization of the hologram aperture; and (b) with apodization.

to note that the mirror used as test object is not a perfectly flat surface (specification  $\lambda/20$ ) and also introduces fluctuations. High-quality mirrors could be used to perform a calibration of the setup.

An important point which remains to be investigated is the possible modification of the transverse resolution of the DHM method which may result

from the modification of the transmittance of the hologram aperture. As already mentioned in Section 2, with the experimental configuration considered here, a decrease of the aperture size should increase the transverse resolution which is defined by the pixel size in the observation plane  $\Delta\xi$  (see Eq. (2)). Preliminary considerations concerning this question can be deduced from the experimental result of Fig. 8 which presents two amplitude-contrast images obtained by numerical reconstruction of a hologram recorded using a resolution test target (USAF 1950) as specimen. Fig. 8(a) presents the result obtained without apodization and Fig. 8(b) with apodization of the hologram aperture. The reconstruction distance is  $d = 30.0$  cm, the aperture size  $L = 4.85$  mm and the wavelength  $\lambda = 632.8$  nm. According to Eq. (2), this corresponds to a resolution limit  $\Delta\xi = 39.1$   $\mu\text{m}$ . In both Fig. 8(a) and 8(b), the smallest resolved

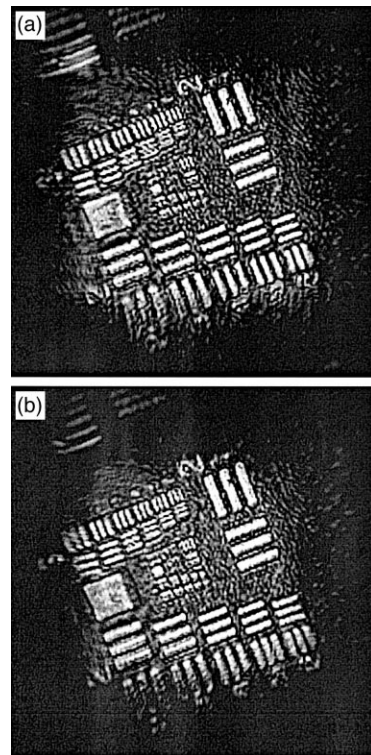


Fig. 8. Amplitude-contrast images obtained by numerical reconstruction of a hologram recorded with a USAF resolution test target as specimen. (a) Without apodization of the hologram aperture; and (b) with apodization.

detail of the test target is element 5 of group 3 which corresponds, according to the specifications of the USAF target, to a resolution of 39.4  $\mu\text{m}$ . We can then conclude that we have a good agreement between the experimentally observed transverse resolution and Eq. (2). We can also conclude that this remark applies for both the image obtained without apodization (Fig. 8(a)) and with apodization (Fig. 8(b)).

The problem of the transverse resolution of the DHM method, in general and in relation with hologram apodization, will be investigated in more details in future works, in particular for the experimental configurations presented in Ref. [8]. The preliminary result presented in Fig. 8 indicates that the apodization of the hologram aperture do not significantly increase the transverse resolution, probably because the apodization procedure does not change the area of the aperture where the transmittance is equal to 0, and because the apodized aperture is completely transparent over a large central area (see Fig. 3).

## 6. Conclusion

It has been established that cubic spline interpolations can be used to design apodized apertures. An attractive feature of this method is that few parameters, four in the present case, are sufficient to define a broad variety of apodization forms. In particular, the shape of the apodization can be optimized by adjusting iteratively the values of these parameters to reach the desired level of fluctuations reduction. Here, an iterative method combining an empirical approach and a automatic approach has been used to perform this optimization. The method is simple to implement and can be used generally in optics for designing apodized apertures.

The potential of the method has been demonstrated by an application to the DHM technique and significant improvements of image quality have been obtained. Regions where diffraction effects becomes negligible have been defined in the center of the reconstructed amplitude-contrast and phase-contrast images. Using a computer generated hologram, we have shown that the standard deviation of the phase

distribution is one order of magnitude smaller in the apodized case than in the unapodized case.

Interesting information concerning the DHM method have been deduced from the obtained results. It has been established that the noise associated to the numerical reconstruction method represents an optical path length of 0.15 nm at a wavelength of 632.8 nm. This result has been obtained numerically and gives an estimation of the resolution limit of the method for phase measurements without experimental sources of noise. A resolution of 5 nm has been deduced from experimental results which have shown that better performances should be easily achieved by optimizing the opto-mechanical design of the apparatus.

## Acknowledgements

This work was supported by the Swiss National Fund for Scientific Research grant 20-49628.96. The authors thank P. Dahlgren for her contribution.

## References

- [1] A.J. Campillo, J.E. Pearson, S.L. Shapiro, N.J. Terrel Jr., Fresnel diffraction effects in the design of high-power laser systems, *Appl. Phys. Lett.* 23 (1973) 85–87.
- [2] G.R. Hadley, Diffraction by apodized aperture, *IEEE J. Quantum Electron.* 10 (1974) 603–608.
- [3] T. Araki, T. Asakura, Coherent apodization problem, *Opt. Commun.* 20 (1977) 373–377.
- [4] J.P. Mills, B.J. Thompson, Effect of aberration and apodization on the performance of coherent optical systems. II. *Imaging, J. Opt. Soc. Am. A* 3 (1986) 704–716.
- [5] Z. Jaroszewicz, J. Sochacki, A. Kolodziejczyk, L.R. Staronki, Apodized annular-aperture logarithmic axicon: smoothness and uniformity of intensity distributions, *Opt. Lett.* 18 (1993) 1893–1895.
- [6] R. Tommasini, F. Löwenthal, J.E. Balmer, H.P. Weber, Iterative method for phase-amplitude retrieval and its application to the problem of beam-shaping and apodization, *Opt. Commun.* 153 (1998) 339–346.
- [7] E. Cuhe, F. Bevilacqua, C. Depeursinge, Digital holography for quantitative phase-contrast imaging, *Opt. Lett.* 24 (1999) 291–293.
- [8] E. Cuhe, P. Marquet, C. Depeursinge, Simultaneous amplitude and quantitative phase-contrast microscopy by numerical reconstruction of Fresnel off-axis holograms, *Appl. Opt.* 38 (1999) 6994–7001.

- [9] J.W. Goodman, R.W. Lawrence, Digital image formation from electronically detected holograms, *Appl. Phys. Lett.* 11 (1967) 77–79.
- [10] U. Schnars, Direct phase determination in hologram interferometry with use of digitally recorded holograms, *J. Opt. Soc. Am. A* 11 (1994) 2011–2015.
- [11] O. Coquoz, R. Conde, F. Taleblou, C. Depeursinge, Performances of endoscopic holography with a multicore optical fiber, *Appl. Opt.* 34 (1995) 7186–7193.
- [12] K. Boyer, J.C. Solem, J.W. Longworth, A.B. Borisov, C.K. Rhodes, Biomedical three-dimensional holographic microimaging at visible, ultraviolet and X-ray wavelength, *Nature Med.* 2 (1996) 939–941.
- [13] E. Cuche, P. Poscio, C. Depeursinge, Optical tomography at the microscopic scale by means of a numerical low coherence holographic technique, in: H.J. Foth, R. Marchesini, H. Pobielska (Eds.), *Optical and Imaging Techniques for Biomonitoring II*, Proc. SPIE 2927, 1996, pp. 61–66.
- [14] T. Zhang, I. Yamaguchi, Three-dimensional microscopy with phase-shifting digital holography, *Opt. Lett.* 23 (1998) 1221–1223.
- [15] D. Beghin, E. Cuche, P. Dahlgren, C. Depeursinge, G. Delacrétaz, R.P. Salathé, Single acquisition polarisation imaging with digital holography, *Electron. Lett.* 35 (1999) 2053–2055.
- [16] W.H. Press, B.P. Flannery, S.A. Teukolski, W.T. Vetterling, *Numerical Recipes*, Cambridge University Press, Cambridge, 1989 (Chapter 10).